

# Dalton Transactions

Accepted Manuscript



This is an *Accepted Manuscript*, which has been through the Royal Society of Chemistry peer review process and has been accepted for publication.

*Accepted Manuscripts* are published online shortly after acceptance, before technical editing, formatting and proof reading. Using this free service, authors can make their results available to the community, in citable form, before we publish the edited article. We will replace this *Accepted Manuscript* with the edited and formatted *Advance Article* as soon as it is available.

You can find more information about *Accepted Manuscripts* in the [Information for Authors](#).

Please note that technical editing may introduce minor changes to the text and/or graphics, which may alter content. The journal's standard [Terms & Conditions](#) and the [Ethical guidelines](#) still apply. In no event shall the Royal Society of Chemistry be held responsible for any errors or omissions in this *Accepted Manuscript* or any consequences arising from the use of any information it contains.

## ARTICLE

# Design, crystal structures and magnetic properties of anionic salts containing fullerene C<sub>60</sub> and indium(III) bromide phthalocyanine radical anions

Cite this: DOI: 10.1039/x0xx00000x

Dmitri V. Konarev,<sup>\*a</sup> Alexey V. Kuzmin,<sup>b</sup> Salavat S. Khasanov,<sup>b</sup> Akihiro Otsuka,<sup>c</sup> Hideki Yamochi,<sup>c</sup> Gunzi Saito<sup>d</sup> and Rimma N. Lyubovskaya<sup>a</sup>

Received 00th January 2012,  
Accepted 00th January 2012

DOI: 10.1039/x0xx00000x

www.rsc.org/

Two salts containing fullerene C<sub>60</sub> and indium(III) bromide phthalocyanine (Pc) radical anions have been obtained as single crystals: (TBA<sup>+</sup>)<sub>3</sub>(C<sub>60</sub><sup>•-</sup>){In<sup>III</sup>(Br)(Pc)<sup>•-</sup>}(Br<sup>-</sup>)·C<sub>6</sub>H<sub>4</sub>Cl<sub>2</sub> (**1**) and (TEA<sup>+</sup>)<sub>2</sub>(C<sub>60</sub><sup>•-</sup>){In<sup>III</sup>(Br)(Pc)<sup>•-</sup>·C<sub>6</sub>H<sub>4</sub>Cl<sub>2</sub>·C<sub>6</sub>H<sub>14</sub> (**2**) where TBA<sup>+</sup> and TEA<sup>+</sup> are tetrabutyl- and tetraethylammonium cations, respectively. The presence of both radical anions is supported by spectra of **1** and **2** in the NIR and IR-ranges. The salts contain zig-zag C<sub>60</sub><sup>•-</sup> chains with 10.136 and 10.383 Å center-to-center (ctc) distances in **1** and a uniform ctc distance of 10.186 Å in **2**. In **1**, the C<sub>60</sub><sup>•-</sup> radical anions are dimerized in the 180-140 K range to form singly bonded (C<sub>60</sub><sup>-</sup>)<sub>2</sub> dimers, whereas they remain monomeric in **2**. Effective packing of planar In(Br)(Pc)<sup>•-</sup> and spherical C<sub>60</sub><sup>•-</sup> is attained by introducing fullerene spheres between the phenylene substituents of Pc allowing the formation of multiple van der Waals contacts between them. Effective magnetic moment of **1** at 300 K is 2.35 μ<sub>B</sub> indicating a contribution of both C<sub>60</sub><sup>•-</sup> and In(Br)(Pc)<sup>•-</sup> species having *S* = 1/2 spin state. There is strong antiferromagnetic coupling of spins between fullerenes in the chains and fullerenes and phthalocyanines in the monomeric phase of **1** with the Weiss temperature of -120 K in the 300-180 K range. The formation of diamagnetic (C<sub>60</sub><sup>-</sup>)<sub>2</sub> dimers switches off magnetic coupling and magnetically isolates In(Br)(Pc)<sup>•-</sup> (Weiss temperature is only -1 K in the 140-10 K range). Magnetic behavior of **2** is described by the Curie-Weiss law with weak ferromagnetic coupling of spins with *θ* = +7.6 K in the 50-300 K range. Both salts manifest single Lorentzian EPR lines at room temperature with *g* = 1.9911 and linewidth (*ΔH*) of 25.4 mT (**1**) and *g* = 1.9956 and *ΔH* = 7.5 mT (**2**) which can be attributed to both C<sub>60</sub><sup>•-</sup> and In(Br)(Pc)<sup>•-</sup> species having strong exchange interaction. An asymmetric signal with the main component at *g* = 1.989-1.965 in the dimeric phase of **1** was attributed to the In(Br)(Pc)<sup>•-</sup> radical anions.

## Introduction

Fullerenes and metal phthalocyanines are wide classes of compounds which can show promising conducting and magnetic properties in ionic states. For example, fullerenes manifest metallic conductivity in the MC<sub>60</sub> salts and some layered complexes, superconductivity in M<sub>3</sub>C<sub>60</sub> salts and form even pure organic ferromagnets with high enough ordering temperature of 19 K.<sup>1-5</sup> These properties are mainly manifested when fullerene has a radical anion state with -1 or -3 charge on the molecule. High conductivity and promising magnetic properties of oxidized metal phthalocyanines are also well known.<sup>6-8</sup> As in fullerenes, the existence of metallic conductivity or even superconductivity was predicted for anionic metal phthalocyanines.<sup>9</sup> However, only several compounds containing negatively charged metal phthalocyanines were obtained and characterized in solid state by now. These compounds were obtained with cobalt(I), iron(I), metal free and magnesium(II) phthalocyanine anions and anions of iron(I) hexadecachlorophthalocyanine.<sup>10-16</sup> Several works are

dedicated to metal phthalocyanines doping by alkali metals<sup>17-19</sup> but no single crystals can be obtained by this method.

A coexistence of metal phthalocyanines and fullerenes in one compound is a very promising task since these compounds can combine unique magnetic, conducting and optical properties of both fullerenes and phthalocyanines. Indeed, in spite of different shapes of these molecules, they can be cocrystallized in one compound.<sup>20-24</sup> Those can be molecular complexes containing neutral fullerenes and phthalocyanines like [Fe<sup>II</sup>Pc(C<sub>5</sub>H<sub>5</sub>N)<sub>2</sub>]·C<sub>60</sub>·4C<sub>6</sub>H<sub>4</sub>Cl<sub>2</sub>.<sup>20</sup> C<sub>60</sub> radical anions also form ionic (C<sub>60</sub><sup>•-</sup>)·(M<sup>II</sup>Pc·L<sup>-</sup>)·(D<sup>+</sup>)<sub>2</sub> complexes with zinc(II), manganese(II) and magnesium(II) phthalocyanines which coordinate negatively charged anions like L = Γ<sup>-</sup>, CH<sub>3</sub>CH<sub>2</sub>S<sup>-</sup> and OH<sup>-</sup>. PMDAE<sup>+</sup> and TMP<sup>+</sup> were used as counter cations D<sup>+</sup> (the cations of *N, N, N, N, N*-pentamethyldiaminoethane and *N, N, N*-trimethylpiperazinium, respectively). No negative charge on metal phthalocyanine has been found in these complexes. Phthalocyanines form π-π stacking {M<sup>II</sup>Pc(L<sup>-</sup>)<sub>2</sub>} dimers, whereas the C<sub>60</sub><sup>•-</sup> radical anions are arranged in layers or chains. In most cases, fullerenes dimerize below 250 K to form diamagnetic singly bonded (C<sub>60</sub><sup>-</sup>)<sub>2</sub>

dimers and only in  $\{\text{Mn}^{\text{II}}\text{Pc}(\text{CH}_2\text{CH}_2\text{S}^-)_x(\Gamma^-)_{1-x}\} \cdot (\text{C}_{60}^{\bullet-}) \cdot (\text{PMDAE}^+)_2 \cdot \text{C}_6\text{H}_4\text{Cl}_2$  ( $x = 0.87$ ) they remain in the monomeric state.<sup>21, 22</sup> Negatively charged fullerenes and metal phthalocyanine anions were for the first time combined in one compound in  $(\text{C}_{70}^-)_2\{(\text{Fe}^{\text{I}}\text{Pc})\}_6(\text{cryptand}(2,2,2))_8[\text{Na}^+]_8$  Solvent, containing fullerene  $\text{C}_{70}$  and iron(I) phthalocyanine anions. However, since the  $\text{C}_{70}^{\bullet-}$  radical anions strongly tend to dimerization, they form diamagnetic singly bonded  $(\text{C}_{70}^-)_2$  dimers at temperature essentially higher than 293 K. As a result, the compound manifests only paramagnetic behavior due to magnetic isolation of paramagnetic  $(\text{Fe}^{\text{I}}\text{Pc})^-$  anions by diamagnetic  $(\text{C}_{70}^-)_2$  dimers, cryptand  $\{2,2,2\} \cdot (\text{Na}^+)$  cations and solvent molecules.<sup>23</sup>

In this work we report the first two salts combining fullerene  $\text{C}_{60}$  and indium(III) bromide phthalocyanine radical anions:  $(\text{TBA}^+)_3(\text{C}_{60}^{\bullet-})\{\text{In}^{\text{III}}(\text{Br})(\text{Pc})^{\bullet-}\}(\text{Br}) \cdot \text{C}_6\text{H}_4\text{Cl}_2$  (**1**) and  $(\text{TEA}^+)_2(\text{C}_{60}^{\bullet-})\{\text{In}^{\text{III}}(\text{Br})(\text{Pc})^{\bullet-}\} \cdot \text{C}_6\text{H}_4\text{Cl}_2 \cdot \text{C}_6\text{H}_{14}$  (**2**), where  $\text{TBA}^+$  and  $\text{TEA}^+$  are tetrabutyl- and tetraethylammonium cations, respectively. We determined crystal structure of these salts and characterized them by IR- and UV-visible-NIR- and EPR spectroscopy, and performed SQUID measurements for **1**. Strong antiferromagnetic coupling of spins between  $\text{C}_{60}^{\bullet-}$  as well as  $\text{C}_{60}^{\bullet-}$  and  $\text{In}(\text{Br})(\text{Pc})^{\bullet-}$  radical anions is shown in **1**, whereas weak ferromagnetic coupling is realized in **2**. Reversible dimerization of  $\text{C}_{60}^{\bullet-}$  in **1** in the 140-180 K range interrupts magnetic interaction between spins and the salt transmits to a paramagnetic state. It should be noted that there are no data on the  $\text{In}(\text{Br})(\text{Pc})^{\bullet-}$  radical anions till now and in this work we present for the first time their molecular structure, optical and magnetic properties.

## Results and discussion

### a). Synthesis

Both fullerene  $\text{C}_{60}$  and metal phthalocyanines can be reduced to the radical anion state by strong reductant sodium fluorenone ketyl in the presence of organic cations like  $\text{TBA}^+$  or  $\text{TEA}^+$ . In contrast to other reduced metal phthalocyanines, indium(III) chloride phthalocyanine does not crystallize as  $\text{TBA}^+$  or  $\text{TEA}^+$  salts by the diffusion of hexane into the solution. That allows the cocrystallization of both anionic fullerene and phthalocyanine components in one compound. The salts, in which the axial chloride anions at the indium(III) atoms are substituted by bromide anions originated from tetraalkylammonium bromide, can be obtained in pure forms allowing one to determine their crystal structures and characterize optical and magnetic properties. Since sodium fluorenone ketyl can generate even fullerene dianions in solution,<sup>25</sup> only two equivalents of the reductant were used for an equimolar fullerene – phthalocyanine mixture.

### b). Optical properties

IR-spectra of salts **1** and **2** are shown in Supporting information (Table S1, Fig. S1). They show IR-active bands of reduced  $\text{C}_{60}$  and  $\text{In}(\text{Br})(\text{Pc})$  along with those of cations and solvent molecules. Some strong intensity bands of  $\text{In}(\text{Cl})(\text{Pc})$  are shifted up to  $5\text{--}10\text{ cm}^{-1}$  at the formation of  $\text{In}(\text{Br})(\text{Pc})^{\bullet-}$  (bands at 724, 771, 1084, 1118, 1332  $\text{cm}^{-1}$  in the spectrum of starting  $\text{In}(\text{Cl})(\text{Pc})$ ). Fullerenes manifest three of four IR-active bands in the spectra of the salts. The  $F_{1u}(4)$   $\text{C}_{60}$  mode which is most sensitive to charge transfer to the  $\text{C}_{60}$  molecule is shifted from 1429  $\text{cm}^{-1}$  (position characteristic of neutral  $\text{C}_{60}$ ) to 1386-1396  $\text{cm}^{-1}$  at the formation of fullerene salts with -1 charge on the molecule.<sup>26-28</sup> The position of this mode in the spectra of **1** and **2** at 1391  $\text{cm}^{-1}$  allows one to assign the charge state of fullerene to -1. The alternation of relative intensities of the  $F_{1u}(1)$  and  $F_{1u}(2)$

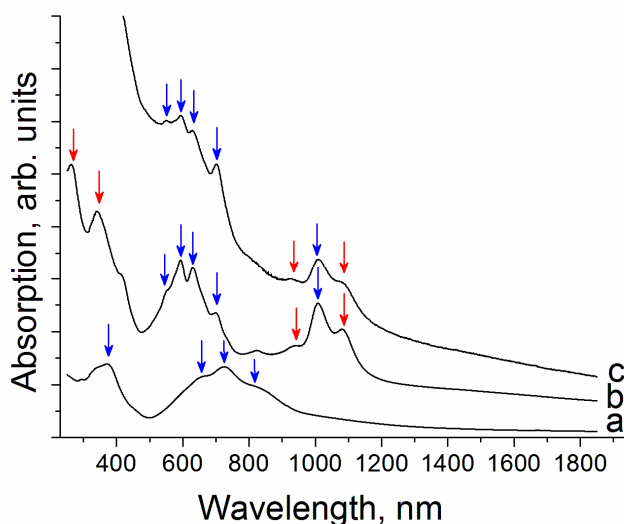


**Figure 1.** UV-visible-NIR spectra for starting  $\text{In}(\text{Cl})(\text{Pc})$  (a) and salts **1** (b) and **2** (c) in KBr pellets prepared in anaerobic conditions for **1** and **2**. The bands attributed to the  $\text{C}_{60}^{\bullet-}$  and  $\text{In}(\text{Br})(\text{Pc})^{\bullet-}$  radical anions are shown by red and blue arrows, respectively.

absorption bands at 516 and 575  $\text{cm}^{-1}$  are also characteristic of negatively charged fullerenes<sup>26-28</sup>.

UV-visible-NIR spectra of the salts (Fig. 1) are very rich. The bands at 262 and 340, 941 and 1080 nm in the spectrum of **1** and at 930 and 1080 nm in the spectrum of **2** can be attributed to  $\text{C}_{60}$  (Fig. 1, red arrows). Two bands in the NIR-range at 930-941 and 1080 nm unambiguously justify radical anion state of fullerenes in **1** and **2** with -1 charge on the molecule.<sup>29-30</sup> Multiple bands at 417 (shoulder), 547, 593, 630, 698 and 1009 nm (**1**) and 550, 593, 626, 702, 1007 nm (**2**) can be attributed to the  $\text{In}(\text{Br})(\text{Pc})^{\bullet-}$  radical anions (Fig. 1, blue arrows). Starting neutral  $\text{In}(\text{Cl})(\text{Pc})$  manifests the Soret band at 370 nm and the split Q-band at 672, 724 and 832 nm (Fig. 1, spectrum a). It is seen that the formation of  $\text{In}(\text{Br})(\text{Pc})^{\bullet-}$  noticeably shifts the Q-band to higher energies and splits into several bands observed at 547-550, 626-630 and 698-702 nm. Another interesting feature is the appearance of a new intense band at 1007-1009 nm in the NIR range at the formation of  $\text{In}(\text{Br})(\text{Pc})^{\bullet-}$  (Fig. 1, spectra b and c). This band is characteristic of phthalocyanine radical anions with electron delocalized on the phthalocyanine macrocycle.<sup>14, 15</sup> For example, in the spectra of the salts with metal free phthalocyanine radical anions ( $\text{H}_2\text{Pc}^{\bullet-}$ ), this band is observed at 1028-1033 nm.<sup>14</sup> It is seen that substitution of two pyrrole hydrogen atoms of  $\text{H}_2\text{Pc}^{\bullet-}$  by the indium bromide fragment in  $\text{In}(\text{Br})(\text{Pc})^{\bullet-}$  only slightly blue shifts this band in the spectra of **1** and **2**. It should be noted that the formation of the  $\text{Fe}^{\text{I}}\text{Pc}^-$  and  $\text{Co}^{\text{I}}\text{Pc}^-$  anions with localization of an additional electron on the metal center is not accompanied by the appearance of new bands in the NIR range.<sup>12, 13, 23</sup> Thus, at the reduction of indium(III) chloride phthalocyanine electron comes to the phthalocyanine macrocycle and indium preserves +3 charge as was predicted from its electrochemistry.<sup>31</sup>

### c). Crystal structures

At 250 K salt **1** contains three  $\text{TBA}^+$  cations and three different types of anions: monomeric  $\text{C}_{60}^{\bullet-}$ ,  $\text{In}(\text{Br})(\text{Pc})^{\bullet-}$  and free bromide ( $\text{Br}^-$ ) anions (Fig. 2a shows these components at 100 K). Thus,  $\text{C}_{60}^{\bullet-}$  and  $\text{In}(\text{Br})(\text{Pc})^{\bullet-}$  radical anions coexist in one compound. For the coexistence of phthalocyanine and fullerene anions in a salt, only one example with dimerized fullerene anions,  $(\text{C}_{70}^-)_2\{(\text{Fe}^{\text{I}}\text{Pc})\}_6(\text{cryptand}[2,2,2] \cdot [\text{Na}^+]_8)$  Solvent has been reported so far.<sup>23</sup>

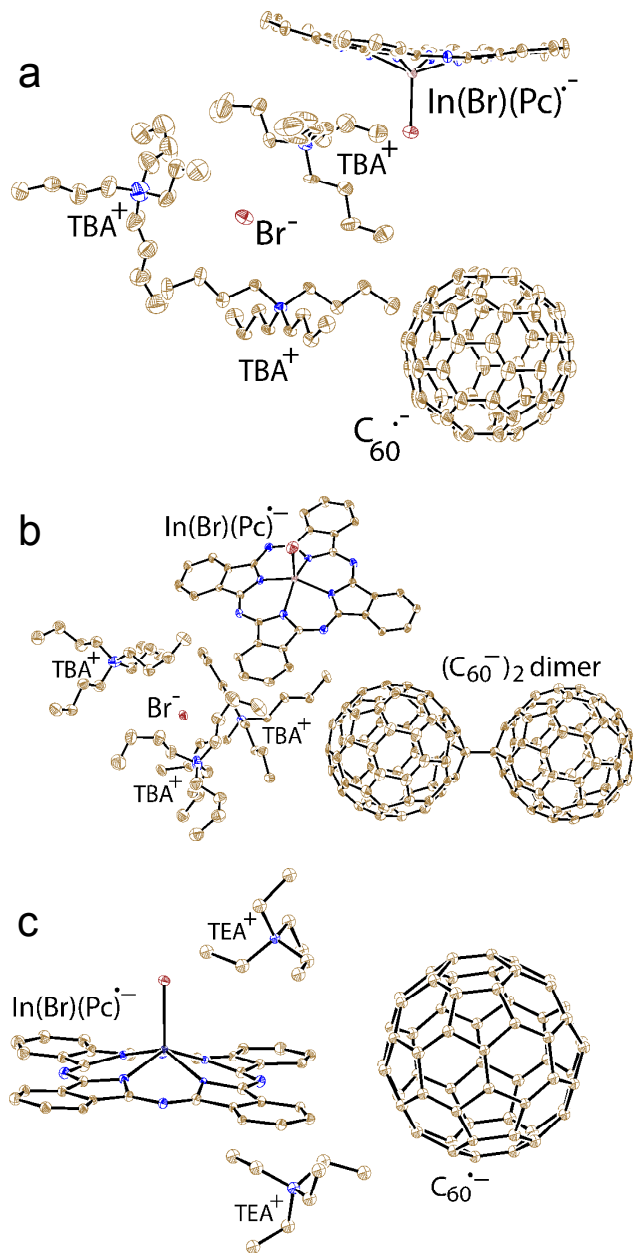


**Figure 2.** Charged components in the crystal structures of **1** at 250 (a) and 100 K (b) and **2** (c) at 90 K. Only major occupied orientations for the disordered components are shown. Ellipsoids are shown with the 50% probability.

Ionic components packing in the crystal structure of **1** is shown in Fig. 3. There are zig-zag fullerene chains in **1** coming along the *b*-axis. These chains are not uniform since center-to-center interfullerene distances are 10.136 and 10.383 Å. The former distance is shorter than the van der Waals (vdW) diameter of  $C_{60}$  (10.18 Å), and vdW C...C contacts are formed between fullerenes. The latter ctc distance is essentially longer than vdW diameter of  $C_{60}$ , and no vdW contacts are formed. Fullerene chains are arranged in the layers separated by the phthalocyanine layers containing  $TBA^+$  cations, free bromide anions and solvent  $C_6H_4Cl_2$  molecules. There are no vdW contacts between  $In(Br)(Pc)^{\bullet-}$  in **1** since they are separated by bulky  $TBA^+$  cations along the *a*-axis (Fig. 3a). However, multiple short vdW C...C contacts are formed between phthalocyanine and fullerene radical anions since fullerene spheres are introduced between phenylene groups of phthalocyanines (Fig.

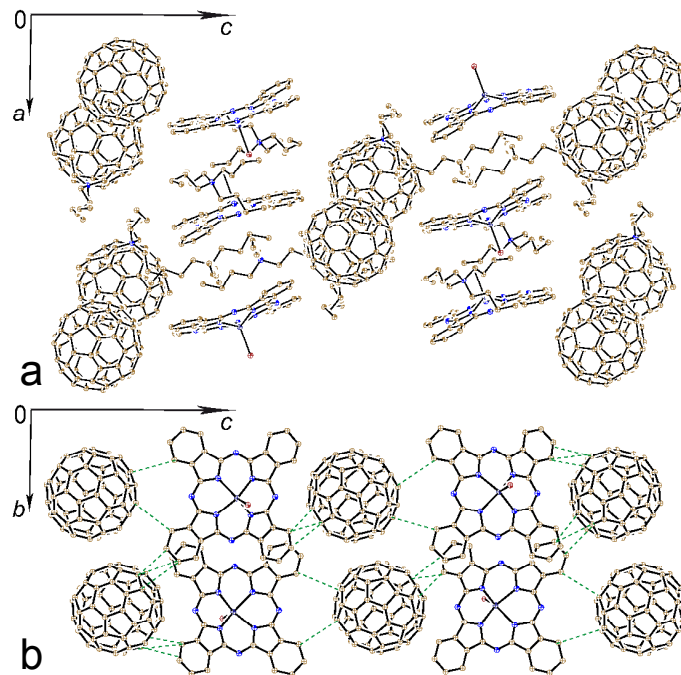


**Figure 3.** Crystal structure of monomeric phase of salt **1** at 250 K viewed along the *b*- (a) and *a*-axes (b).  $In(Br)(Pc)^{\bullet-}$  units are located far from each other in Fig. b since they are separated by  $TBA^+$  cations along the *a*-axis (as shown in Fig. a). Bromide anions and solvents molecules are not shown.

3b, vdW C...C contacts are shown by green dashed lines). Contacts are short enough (3.47-3.68 Å) to provide effective magnetic coupling between these two paramagnetic species.

Crystal structure of **1** solved at 100 K indicates dimerization of  $C_{60}^{\bullet-}$  and the formation of singly bonded  $(C_{60}^{\bullet-})_2$  dimers (Fig. 2a). The dimers are formed in fullerene zig-zag chains namely in the fullerene pairs with the shorter center-to-center distance of 10.136 Å. The dimers are well ordered allowing one to determine the interdice C-C bond length of 1.593(17) Å and the ctc distance between fullerenes in the dimers of 9.292 Å. These values are in the range of values found previously for singly bonded  $(C_{60}^{\bullet-})_2$  dimers.<sup>32-39</sup>

Salt **2** contains two  $TEA^+$  cations and two types of anions: a monomeric  $C_{60}^{\bullet-}$  radical anion and a  $In(Br)(Pc)^{\bullet-}$  radical anion (Fig. 2b). The main structural motif of salt **2** is zig-zag fullerene chains arranged parallel to the *c*-axis (Fig. 4a). The ctc interfullerene distance in the chain is uniform and rather long (10.186 Å). That does not allow the dimerization of  $C_{60}^{\bullet-}$ . Fullerene chains are separated by phthalocyanines.  $TEA^+$  cations are located in the cavities formed in zig-zag fullerene chains in which phenylene groups of phthalocyanines are inserted as well. As a result, two negatively charged components are held together in a crystal by the  $TEA^+$  cations.

$In(Br)(Pc)^{\bullet-}$  and a couple of  $C_{60}^{\bullet-}$  are alternatively arranged along the *c*-axis to form an anion ribbon, in which each  $In(Br)(Pc)^{\bullet-}$  is surrounded by four  $C_{60}^{\bullet-}$  (Fig. 4b). However, in this case, the number of van der Waals contacts is smaller and they are longer (3.56-3.80 Å) than those in **1**. That should result in the weaker magnetic interactions in **2** than those in **1**. Two ribbons of  $In(Br)(Pc)^{\bullet-}$  and  $C_{60}^{\bullet-}$  are connected by additional  $In(Br)(Pc)^{\bullet-}$  to form a vacancy which accommodates  $TEA^+$  cations and solvent molecules (Fig. 4c).

Molecular geometry of ordered  $In(Br)(Pc)^{\bullet-}$  radical anions has been determined for the first time in salt **1** at 100 K. The average equatorial In-N(Pc) bond length is 2.136(6) Å, the

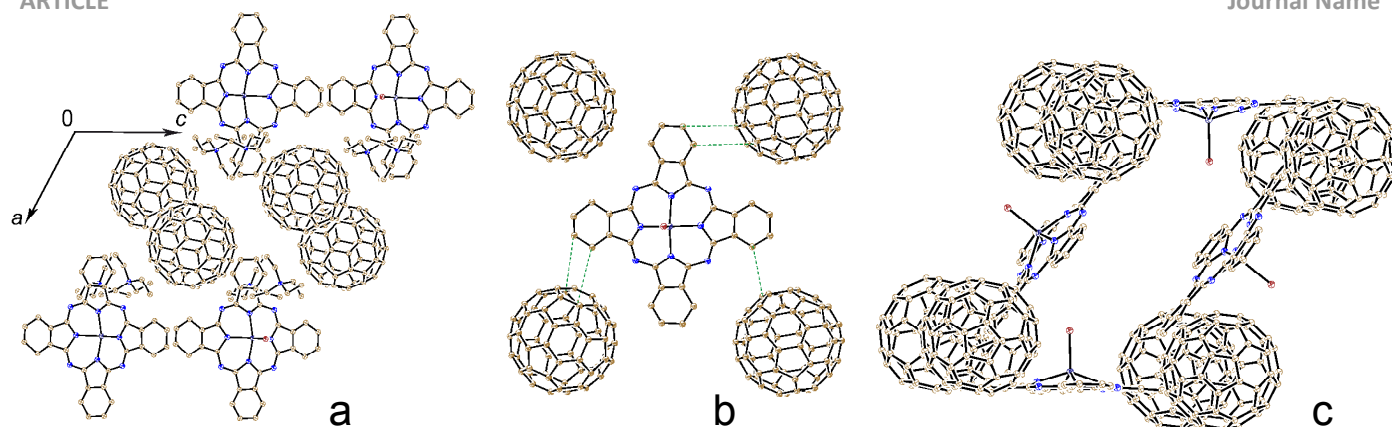


**Figure 4.** View on the fragment of crystal structure of salt **2** along the *b*-axis (a); main building block of salt **2** in which one  $\text{In}(\text{Br})(\text{Pc})^{\bullet-}$  radical anion is surrounded by four  $\text{C}_{60}^{\bullet-}$  (van der Waals C...C contacts are shown by green dashed lines) (b); large cavity formed by four  $\text{In}(\text{Br})(\text{Pc})^{\bullet-}$  - 4  $\text{C}_{60}^{\bullet-}$  units are occupied by  $\text{TEA}^+$  cations and solvent molecules (c).

displacement of indium atom from the 24-atom phthalocyanine plane towards the bromide anion is 0.896 Å and the length of axial In-Br bonds is 2.604(1) Å at 100 K. The structure of neutral indium(III) bromide phthalocyanine is unknown and a comparison with neutral indium(III) iodide phthalocyanine can only be made. In this case the average equatorial In-N bond length is 2.130(6) Å, the axial In-Br bond length is 2.672(2) Å

and the displacement of indium atom from the 24-atom phthalocyanine plane towards the iodide anion is 0.839 Å.<sup>40</sup> It seems that the reduction of macrocycle to form of  $\text{In}(\text{Br})(\text{Pc})^{\bullet-}$  is accompanied by slightly stronger displacement of indium atoms from the 24-atom phthalocyanine plane towards bromide anions whereas averaged In-N(Pc) bonds are only slightly longer in  $\text{In}(\text{Br})(\text{Pc})^{\bullet-}$  (however, this elongation is within experimental error).

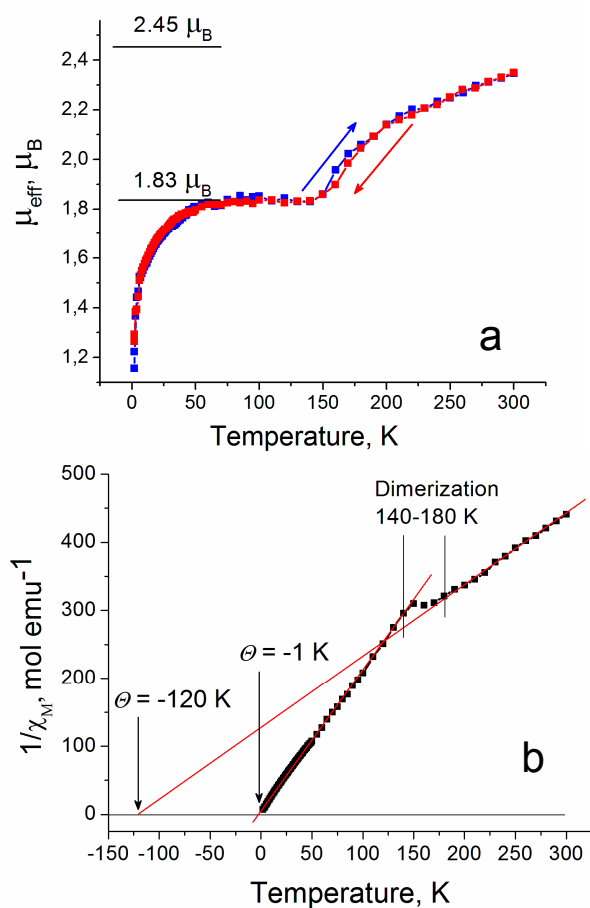


**Figure 5.** Magnetic properties for salt **1** measured by SQUID: temperature dependence of effective magnetic moment measured in heating (blue squares) and cooling (red squares) conditions (a) and reciprocal molar magnetic susceptibility (b) of polycrystalline **1**.

#### d). Magnetic properties

Magnetic properties of **1** were studied by SQUID and EPR techniques. Effective magnetic moment is 2.35  $\mu_B$  at 300 K. That is close to the contribution of two  $S = 1/2$  spins per formula unit (calculated magnetic moment is 2.45  $\mu_B$ ) (Fig. 5a). Thus, both paramagnetic  $\text{In}(\text{Br})(\text{Pc})^{\bullet-}$  and  $\text{C}_{60}^{\bullet-}$  species contribute to the magnetic moment at high temperature. The temperature dependence of reciprocal molar magnetic susceptibility of **1** is shown in Fig. 5b. This dependence is linear in a high-temperature 180-300 K range allowing one to determine Weiss temperature of about -120 K that indicates strong antiferromagnetic coupling of spins in the monomeric phase. The strong antiferromagnetic coupling should be the origin for smaller value of magnetic moment of 1.83  $\mu_B$  at 300 K in comparison with that for the two independent  $S = 1/2$  spins and the decrease of magnetic moment of **1** even below 300 K (Fig. 5a). Two types of interactions can contribute to strong antiferromagnetic coupling of spins observed in **1**. That is magnetic coupling in the  $\text{C}_{60}^{\bullet-}$  chains and coupling between spins localized on  $\text{In}(\text{Br})(\text{Pc})^{\bullet-}$  and  $\text{C}_{60}^{\bullet-}$  whereas the  $\text{In}(\text{Br})(\text{Pc})^{\bullet-}$  radical anions are located far from each other in **1**. There are several compounds which contain layers of  $\text{C}_{60}^{\bullet-}$  with an etc distance of about 10.13 Å or even shorter but Weiss temperature does not usually exceed -30 K.<sup>41,42</sup> Enhanced magnetic coupling is most probably due to additional magnetic interaction between  $\text{In}(\text{Br})(\text{Pc})^{\bullet-}$  and  $\text{C}_{60}^{\bullet-}$  spins.

Judging from the precipitous reduction of magnetic moment (Fig. 5a) and integral intensity of EPR signal (Fig. 7c) as well as transition in the reciprocal molar magnetic susceptibility (Fig. 5b), the dimerization of  $\text{C}_{60}^{\bullet-}$  to form diamagnetic singly bonded  $(\text{C}_{60})_2$  dimers is realized in the 180-140 K range and the magnetic moment is only 1.83  $\mu_B$  below 140 K (Fig. 5a). This value is close to 1.73  $\mu_B$  calculated for the system with one non-interacting  $S = 1/2$  spin and is supposed to originate from remaining  $\text{In}(\text{Br})(\text{Pc})^{\bullet-}$ . Low-temperature dimeric phase is characterized by very small Weiss temperature of -1 K in the 140-10 K range indicating that dimerization of  $\text{C}_{60}^{\bullet-}$  switches off strong antiferromagnetic coupling of spins and

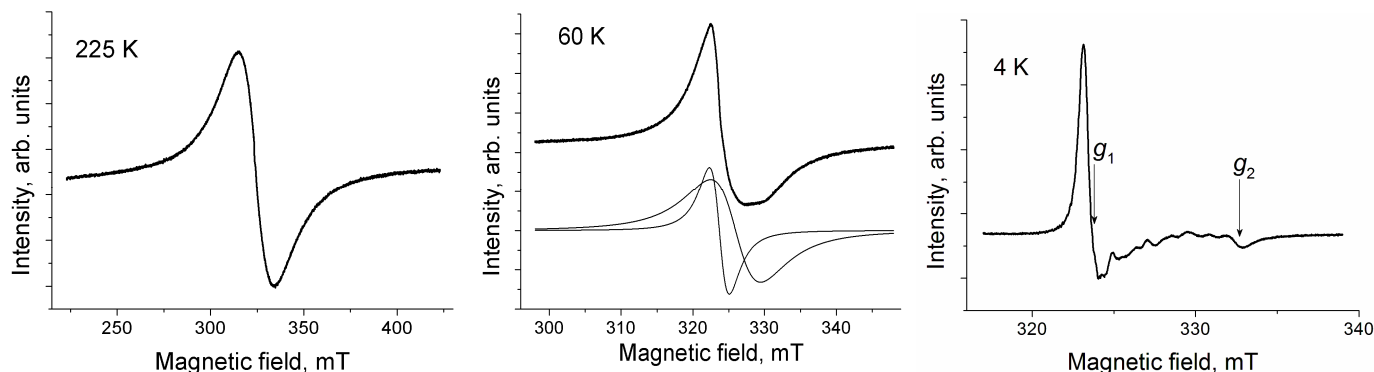


Figure 6. Evolution of EPR signal for polycrystalline **1** with temperature. Spectra at 225, 60 and 4 K are shown.

magnetically isolated  $\text{In}(\text{Br})(\text{Pc})^{\bullet-}$  radical anions are formed. Since dimerization is reversible (only with small hysteresis, Fig. 5a), the transition from strong to weak magnetic coupling of spins also occurs completely reversibly.

The EPR signal of **1** is a broad Lorentzian line with  $g$ -factor of 1.9911 and linewidth ( $\Delta H$ ) of 25.4 mT (Fig. 6 shows this signal at 225 K). This signal is noticeably different from those observed for the  $\text{C}_{60}^{\bullet-}$  radical anions, which generally have  $g$ -factors in the 1.996–2.000 range and are essentially narrower ( $\Delta H = 2\text{--}8$  mT at room temperature).<sup>28–30</sup> Thus, the observed signal can be attributed to both paramagnetic  $\text{In}(\text{Br})(\text{Pc})^{\bullet-}$  and  $\text{C}_{60}^{\bullet-}$  species showing strong exchange magnetic interaction. Generally, in this case the Lorentzian signal with an intermediate  $g$ -factor value between those characteristic of individual species is manifested.<sup>30</sup> Therefore, we can suppose that the EPR signal from  $\text{In}(\text{Br})(\text{Pc})^{\bullet-}$  should have  $g$ -factor lower than 1.991.  $g$ -factor of the signal only slightly decreases, and the signal narrows with the temperature decrease (Fig. 7a and b). Dimerization of  $\text{C}_{60}^{\bullet-}$  realized in the 140–180 K range is accompanied by the decrease of integral intensity of the signal to the half (Fig. 7c). Since diamagnetic singly bonded  $(\text{C}_{60}^-)_2$  dimers are EPR silent,<sup>32–39</sup> we can suppose that the EPR signal below 140 K originates mainly from  $\text{In}(\text{Br})(\text{Pc})^{\bullet-}$ . The signal attributed to  $\text{In}(\text{Br})(\text{Pc})^{\bullet-}$  is split into two components below 140 K (Fig. 6, spectrum at 60 K). The main component has  $g$ -factor of 1.9890 and  $\Delta H = 14.50$  mT at 120 K. At the beginning, the second component with  $g_2 = 1.9965$  ( $\Delta H = 4.55$  mT) has very weak intensity of  $\sim 4\%$  from that of the main component (at 120 K). However, the contribution of the second component increases with the temperature decrease and is about 50% from that of the main signal at 40 K. On the whole, both components of the EPR signal attributed to  $\text{In}(\text{Br})(\text{Pc})^{\bullet-}$  strongly narrow with the temperature decrease and their  $g$ -factors are shifted to lower values below 100 K. Below 10 K salt **1** shows a complicate signal with two main components at  $g_1 = 1.9986$

and  $g_2 = 1.9445$ . Split and weak signals are also observed in magnetic fields from 324 up to 332 mT. Signal separation varies in the 0.8–1.4 mT range at 4 K (Fig. 6, spectrum at 4 K). Such splitting can be associated with hyperfine interaction of unpaired spins with  $\text{In}^{115}$  having nuclear spin 9/2 and quadrupole moment,  $Q = 0.86$ . Another more probable reason for the appearance of weak components in the 324–332 mT range is strong asymmetry of  $g_1$ -component of the EPR signal because of polycrystallinity of the sample. Such effects were observed in some anionic fullerene and phthalocyanine compounds containing  $\text{Cp}^*\text{Cr}^+$ ,  $(\text{MDABCO}^+)_2\text{Mn}^{\text{II}}\text{TPP}$  cations or in the salt with the  $(\text{Fe}^{\text{I}}\text{Cl}_{16}\text{Pc})^-$  anions ( $\text{Cp}^*\text{Cr}$  is decamethylchromocene,  $\text{MDABCO}^+$  is *N*-methyl diazabicyclooctanium cation and  $(\text{Fe}^{\text{I}}\text{Cl}_{16}\text{Pc})^-$  is the anion of iron(I) hexadecachlorophthalocyanine).<sup>32, 43, 44</sup> It is interesting that the EPR signal from  $\text{In}(\text{Br})(\text{Pc})^{\bullet-}$  is strongly different from those of the radical anions of metal-free phthalocyanine ( $\text{H}_2\text{Pc}^{\bullet-}$ ) which are essentially narrower ( $\Delta H = 0.1\text{--}0.3$  mT) and have  $g$ -factors of 2.0035–2.0037.<sup>14</sup> Thus, the substitution of hydrogens by a indium-halide fragment strongly affects the EPR spectra of radical anions of these phthalocyanines.

The EPR signal of **2** shows one Lorentzian line with  $g = 1.9956$  and  $\Delta H = 7.5$  mT at room temperature (Fig. 8a shows the EPR signal at 200 K).  $g$ -factor of the signal slightly shifts to lower values and the signal narrows with the temperature decrease (Supporting information, Figs. S2a and S2b). Below 170 K the signal splits into two components which have  $g_1 = 1.9914$  and  $\Delta H = 3.42$  mT and  $g_2 = 1.9985$  and  $\Delta H = 2.43$  mT at 140 K (Fig. 8b shows the EPR signal at 30 K). The temperature dependence of integral intensity of the EPR signal in **2** can be fitted well by the Curie-Weiss expression with positive Weiss temperature of +7.6 K indicating weak ferromagnetic interaction of  $\text{In}(\text{Br})(\text{Pc})^{\bullet-}$  and  $\text{C}_{60}^{\bullet-}$  spins (Supporting information, Fig. S2c). Weak magnetic interactions can be a result of longer distances between  $\text{C}_{60}^{\bullet-}$  in the chains and between  $\text{In}(\text{Br})(\text{Pc})^{\bullet-}$  and  $\text{C}_{60}^{\bullet-}$  species in the crystal structure of **2**.

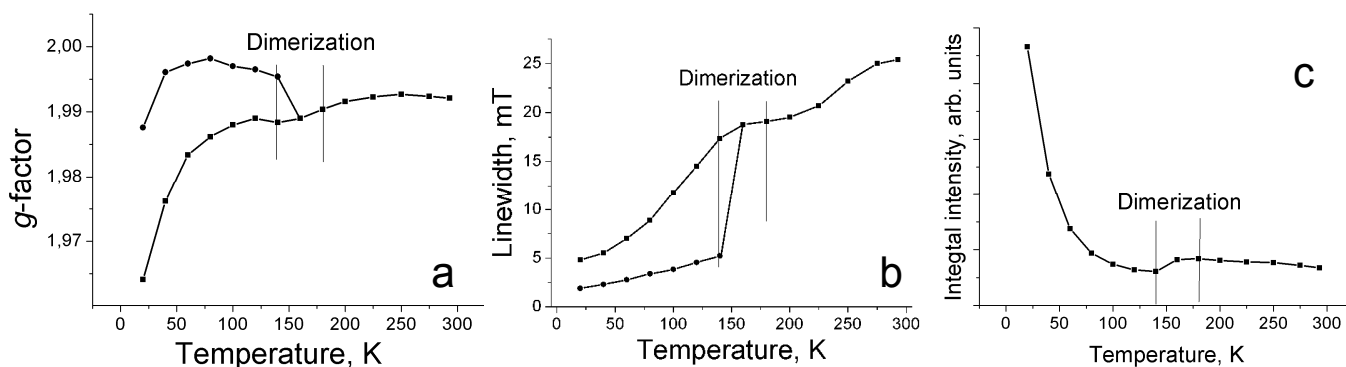


Figure 7. Temperature dependencies of parameters of EPR signal for polycrystalline **1**:  $g$ -factor (a), linewidth (b) and integral intensity (c).

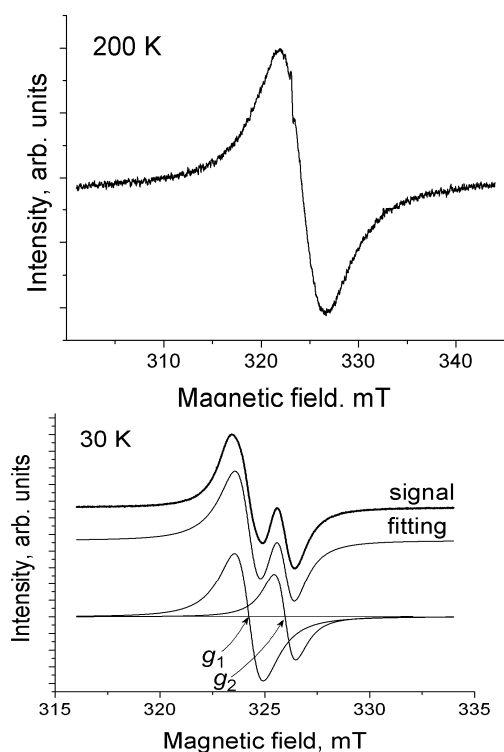


Figure 8. EPR spectrum of polycrystalline **2** measured at 200 and 30 K.

## Experimental

### Materials

$\text{In}^{\text{III}}(\text{Cl})(\text{Pc})$  of 90% purity was purchased from Aldrich, TEABr and TBABr of 98% purity were purchased from TCI.  $\text{C}_{60}$  of 99.98% purity was purchased from MTR Ltd. Sodium fluorenone ketyl was obtained as previously described.<sup>45</sup> All manipulations for the synthesis of **1** and **2** were carried out in a MBraun 150B-G glove box with controlled atmosphere containing  $\text{H}_2\text{O}$  and  $\text{O}_2$  less than 1 ppm. Solvents were purified in argon atmosphere. *o*-Dichlorobenzene ( $\text{C}_6\text{H}_4\text{Cl}_2$ ) was distilled over  $\text{CaH}_2$  under reduced pressure, benzonitrile ( $\text{C}_6\text{H}_5\text{CN}$ ) was distilled over Na under reduced pressure, hexane was distilled over Na/benzophenone. The crystals of **1** and **2** were stored in a glove box. KBr pellets for measurements of IR- and UV-visible-NIR spectra were also prepared in a glove box. EPR (for **1** and **2**) and SQUID (for **1**) magnetic measurements were performed on polycrystalline samples sealed in 2 mm quartz tubes under  $10^{-3}$  Torr.

### Synthesis

The crystals of  $(\text{TBA}^+)_3(\text{C}_{60}^{\bullet-})\{\text{In}^{\text{III}}(\text{Br})(\text{Pc})^{\bullet-}\}(\text{Br}^-)\cdot\text{C}_6\text{H}_4\text{Cl}_2$  (**1**) were obtained by the reduction of 27.6 mg of  $\text{In}^{\text{III}}(\text{Cl})(\text{Pc})$  (0.044 mmol),  $\text{C}_{60}$  (30 mg, 0.044 mmol) in the presence of an excess of TBABr (50 mg, 0.155 mmol) by about two molar equivalents of sodium fluorenone ketyl (20 mg, 0.098 mmol) in 16 ml of *o*-dichlorobenzene at  $100^\circ\text{C}$  during four hours in anaerobic condition. The solution color changed from violet to deep blue and all components completely dissolved. The solution was cooled down to room temperature and stirred overnight. Then it was filtered in a 50 mL glass tube of 1.8 cm diameter with a ground glass plug, and 30 mL of hexane was layered over the solution. The crystals of the salts

were precipitated during 1.5 month. The solvent was decanted off from the crystals and they were washed with hexane. Crystals of **1** were up to  $0.4 \times 0.8 \times 1 \text{ mm}^3$  in size and were obtained with 34% yield. The analysis of the obtained crystals under microscope in a glove box showed the presence of only one phase - black elongated plates of **1** whose composition was determined from X-ray diffraction on single crystal and was confirmed by elemental analysis. Found: C = 72.89, H = 5.24, N = 6.36 %; calc.: C = 73.61, H = 5.37, N = 6.50 %.

The crystals of  $(\text{TEA}^+)_2(\text{C}_{60}^{\bullet-})\{\text{In}^{\text{III}}(\text{Br})(\text{Pc})^{\bullet-}\}\cdot\text{C}_6\text{H}_4\text{Cl}_2\cdot\text{C}_6\text{H}_{14}$  (**2**) were obtained by a similar procedure. Instead of TBABr, an excess of the TEABr salt (36 mg, 0.171 mmol) was used, and 3 ml of benzonitrile was added to increase the solubility of the salt. Diffusion of hexane during 1.5 month produced crystals on the walls of the tube. The solvent was decanted off from the crystals and they were washed with hexane. Crystals of **2** were up to  $0.2 \times 0.5 \times 1 \text{ mm}^3$  in size and were obtained with 28% yield. The analysis of the obtained crystals under microscope in a glove box showed the presence of only one phase, namely, black elongated plates of **2** whose composition was determined from X-ray diffraction on single crystal and was confirmed by elemental analysis. Found: C = 74.38, H = 3.77, N = 7.19 %; calc.: C = 75.00, H = 3.85, N = 7.33 %.

### General

UV-visible-NIR spectra were measured in KBr pellets with a Perkin Elmer Lambda 1050 spectrometer in the 250-2500 nm range. FT-IR spectra were obtained in KBr pellets with a Perkin-Elmer Spectrum 400 spectrometer ( $400\text{-}7800 \text{ cm}^{-1}$ ). EPR spectra were recorded for sealed polycrystalline samples of **1** and **2** from 4 up to 295 K with a JEOL JES-TE 200 X-band ESR spectrometer equipped with a JEOL ES-CT470 cryostat. A Quantum Design MPMS-XL SQUID magnetometer was used to measure static magnetic susceptibility of **1** at 100 mT magnetic field in cooling and heating conditions in the 300 - 1.9 K range. A sample holder contribution and core temperature independent diamagnetic susceptibility ( $\chi_d$ ) were subtracted from the experimental values. The  $\chi_d$  values for **1** ( $\chi_0 = -1412 \times 10^{-6} \text{ emu}\cdot\text{mol}^{-1}$ ) were calculated using the Pascal constants. The values of  $-252 \times 10^{-6} \text{ emu}\cdot\text{mol}^{-1}$  for  $\text{C}_{60}^{46-}$ ,  $-344 \times 10^{-6} \text{ emu}\cdot\text{mol}^{-1}$  for  $\text{In}(\text{Br})\text{Pc}$ ,  $-207 \times 10^{-6} \text{ emu}\cdot\text{mol}^{-1}$  for  $\text{TBA}^+$ ,  $-83 \times 10^{-6} \text{ emu}\cdot\text{mol}^{-1}$  for  $\text{C}_6\text{H}_4\text{Cl}_2$  and  $-77 \times 10^{-6} \text{ emu}\cdot\text{mol}^{-1}$  for  $\text{C}_6\text{H}_{14}$  were used. The values of  $\Theta$  and  $C$  for **1** below and above dimerization were calculated using experimental data in the 10-140 and 180-300 K range using expression  $\chi_M = C/(T-\Theta) + \chi_d$ . Effective magnetic moment ( $\mu_{\text{eff}}$ ) was calculated with formula:  $\mu_{\text{eff}} = (8\chi_M T)^{1/2}$ .

### Crystal structure determination

**Crystal data for 1 at 100 K.**  $\text{C}_{146}\text{H}_{128}\text{Cl}_2\text{Br}_2\text{InN}_{11}$ ,  $M_r = 2382.13 \text{ g mol}^{-1}$ , black plate, monoclinic,  $P 2_1/n$ ,  $a = 15.9670(13)$ ,  $b = 17.4625(14)$ ,  $c = 39.938(3) \text{ \AA}$ ,  $\beta = 90.3410(10)^\circ$ ,  $V = 11135.5(16) \text{ \AA}^3$ ,  $Z = 4$ ,  $d_{\text{calc}} = 1.421 \text{ g}\cdot\text{cm}^{-3}$ ,  $\mu = 1.040 \text{ mm}^{-1}$ ,  $F(000) = 4936$ ,  $2\theta_{\text{max}} = 49.67^\circ$ , reflections measured 76936, unique reflections 19169, reflections with  $I > 2\sigma(I) = 12211$ , parameters refined 1690, restraints 2092,  $R_1 = 0.0844$ ,  $wR_2 = 0.2130$ , G.O.F. = 1.032.

**Crystal data for 1 at 250 K.**  $\text{C}_{146}\text{H}_{128}\text{Cl}_2\text{Br}_2\text{InN}_{11}$ ,  $M_r = 2382.13 \text{ g mol}^{-1}$ , black plate, monoclinic,  $P 2_1/n$ ,  $a = 16.275(1)$ ,  $b = 17.518(1)$ ,  $c = 40.243(2) \text{ \AA}$ ,  $\beta = 90.874(1)^\circ$ ,  $V = 11472.2(11) \text{ \AA}^3$ ,  $Z = 4$ ,  $d_{\text{calc}} = 1.379 \text{ g}\cdot\text{cm}^{-3}$ ,  $\mu = 1.010 \text{ mm}^{-1}$ ,  $F(000) = 4936$ ,  $2\theta_{\text{max}} = 34.514^\circ$ , reflections measured 37908, unique reflections 6962, reflections with  $I > 2\sigma(I) = 5672$ , parameters refined 3049, restraints 5584,  $R_1 = 0.0809$ ,  $wR_2 = 0.2209$ , G.O.F. = 1.047.

**Crystal data for 2 at 90 K.**  $\text{C}_{120}\text{H}_{74}\text{BrCl}_2\text{InN}_{10}$ ,  $M_r = 1921.52 \text{ g mol}^{-1}$ , black block, monoclinic,  $P 2_1/c$ ,  $a = 22.3081(5)$ ,  $b = 16.9276(4)$ ,  $c = 24.9563(5) \text{ \AA}$ ,  $\beta = 115.282(1)^\circ$ ,  $V = 8521.4(3) \text{ \AA}^3$ ,  $Z$

= 4,  $d_{\text{calc}} = 1.498 \text{ g}\cdot\text{cm}^{-3}$ ,  $\mu = 0.873 \text{ mm}^{-1}$ ,  $F(000) = 3928$ ,  $2\theta_{\text{max}} = 52.744^\circ$ , reflections measured 54020, unique reflections 17342, reflections with  $I > 2\sigma(I) = 7971$ , parameters refined 1717, restraints 3038,  $R_1 = 0.1349$ ,  $wR_2 = 0.4274$ , G.O.F. = 1.243.

X-ray diffraction data for **1** at 100 and 250 K (both experiments were carried out for one single crystal at the beginning at 100 and finally at 250 K) and **2** at 90 K were collected on a Bruker Smart Apex II CCD with graphite monochromated MoK $\alpha$  radiation using a Japan Thermal Engineering Co. cooling system DX-CS190LD. Raw data reduction to  $F^2$  was carried out using Bruker SAINT.<sup>47</sup> The structures were solved by direct method and refined by the full-matrix least-squares method against  $F^2$  using WINGX and SHELX-2013 programs.<sup>48, 49</sup> Non-hydrogen atoms were refined in the anisotropic approximation. Positions of hydrogen atoms were calculated geometrically.

### Disorder and peculiarities in the refinement of the crystal structures of **1** and **2**

Crystal structure of **1** at 250 K involves three crystallographically independent TBA<sup>+</sup> cations, one each of C<sub>60</sub><sup>•-</sup>, In(Br)(Pc)<sup>•-</sup>, bromide (Br<sup>-</sup>) anion and solvent C<sub>6</sub>H<sub>4</sub>Cl<sub>2</sub> molecule. The C<sub>60</sub><sup>•-</sup> radical anions are strongly disordered between four orientations with 0.175(9)/0.176(9)/0.295(9)/0.354(9) occupancies. Butyl substituents of one of three TBA<sup>+</sup> cations are also disordered between two positions having 0.604(17)/0.396(17) occupancies. Since single crystal of **1** weakly reflects at 250 K, the reflections are observed only at low angles (the theta cutoff is 17.25°) and low resolution and poor data/parameters ratio are observed for the monomeric phase of **1**. Temperature decrease can solve this problem but noticeable temperature decrease is impossible with the preservation of monomeric phase.

Crystal structure of **1** at 100 K contains three crystallographically independent TBA<sup>+</sup> cations, half of singly bonded completely ordered (C<sub>60</sub>)<sub>2</sub> dimer, one each of In<sup>III</sup>(Br)(Pc)<sup>•-</sup>, bromide (Br<sup>-</sup>) anion and a solvent C<sub>6</sub>H<sub>4</sub>Cl<sub>2</sub> molecule. One of three TBA<sup>+</sup> cations shows the positional disorder of butyl groups with the 0.730(5)/0.270(5) occupancies. The C<sub>6</sub>H<sub>4</sub>Cl<sub>2</sub> molecule is disordered between two orientations with the 0.865(6)/0.135(6) occupancies. The bromine anion has two closely located positions with the 0.880(6)/0.120(6) occupancies. Space occupied by two C<sub>60</sub><sup>•-</sup> decreases after dimerization and that can result in additional disorder of some components in the dimeric phase (C<sub>6</sub>H<sub>4</sub>Cl<sub>2</sub> and bromide anions).

Salt **2** contains two TEA<sup>+</sup> cations and two types of anions: monomeric C<sub>60</sub><sup>•-</sup> radical anion disordered between two orientations with the 0.758(9)/0.242(9) occupancies and In(Br)(Pc)<sup>•-</sup> radical anion. One of two TEA<sup>+</sup> cations is also disordered between two orientations with the 0.559(12)/0.441(12) occupancies. This complex contains two cavities to accommodate solvent molecules. One of them contains well-ordered C<sub>6</sub>H<sub>4</sub>Cl<sub>2</sub> molecule, while second large cavity accommodates strongly disordered solvent molecules. It obviously contains hexane but probably also strongly disordered C<sub>6</sub>H<sub>4</sub>Cl<sub>2</sub> molecule is encapsulated while the positions cannot be specified. Additional electron density peaks are also observed near bromide anions of In(Br)(Pc)<sup>•-</sup>. The position of In and Br above and below the phthalocyanine plane has the 0.556(2)/0.444(2) occupancies. Therefore, when the In-Br fragment is absent, large void is formed which can be occupied by solvent molecules (hexane, C<sub>6</sub>H<sub>4</sub>Cl<sub>2</sub> or C<sub>6</sub>H<sub>5</sub>CN). Due to large size of the cavity, solvent molecules are strongly disordered in them. As a result of small electron density, the positions of solvent molecules cannot be resolved reasonably. All these factors result in a rather high *R*-factor value for this structure ( $R_1 = 0.1349$ ). Nevertheless, the positions of

C<sub>60</sub><sup>•-</sup> radical anion, phthalocyanine and the TEA<sup>+</sup> cations in **2** are solved and refined stably.

For the disordered parts in the crystal structures of **1** and **2**, all distances were calculated and figures are shown for major occupied orientations only. To keep geometry of disordered fullerene, solvent and TBA<sup>+</sup> or TEA<sup>+</sup> cations close to ideal one, the bond length restraints were applied along with the next-neighbour distances using the SADI and SAME SHELXL instructions. That resulted in a great number of restraints used for the refinement of the crystal structures of **1** at 250 and 100 K and **2** at 100 K.

### Conclusions

We obtained two new salts containing simultaneously fullerene C<sub>60</sub> and indium(III) bromide phthalocyanine radical anions: (TBA<sup>+</sup>)<sub>3</sub>(C<sub>60</sub><sup>•-</sup>){In<sup>III</sup>(Br)(Pc)<sup>•-</sup>}(Br<sup>-</sup>)·C<sub>6</sub>H<sub>4</sub>Cl<sub>2</sub> (**1**) and (TEA<sup>+</sup>)<sub>2</sub>(C<sub>60</sub><sup>•-</sup>){In<sup>III</sup>(Br)(Pc)<sup>•-</sup>·C<sub>6</sub>H<sub>4</sub>Cl<sub>2</sub>·C<sub>6</sub>H<sub>14</sub> (**2**). The presence of both radical anions is well proved by their IR- and NIR-spectra. The salts contain zig-zag C<sub>60</sub><sup>•-</sup> chains in both salts. Effective packing of planar In(Br)(Pc)<sup>•-</sup> and spherical C<sub>60</sub><sup>•-</sup> radical anions is attained due to the introduction of fullerene spheres between phenylene substituents of In(Br)(Pc)<sup>•-</sup> allowing the formation of multiple van der Waals contacts between them. The presence of C<sub>60</sub><sup>•-</sup> chains and effective In(Br)(Pc)<sup>•-</sup> and C<sub>60</sub><sup>•-</sup> interactions results in strong antiferromagnetic coupling of spins in **1** and less effective but ferromagnetic coupling of spins in **2**. It should be noted that the reversible dimerization of C<sub>60</sub><sup>•-</sup> in **1** in the 180-140 K range switches off strong magnetic coupling of spins and isolates In<sup>III</sup>(Br)(Pc)<sup>•-</sup> radical anions magnetically. Since dimerization is realized reversibly, the transition from strong to weak magnetic coupling of spins also occurs completely reversibly. The experimental data show that effective magnetic coupling between fullerene and metal phthalocyanine radical anions can realize in spite of different shapes of these anions. The approach to incorporate different anion radical species in a crystal will provide the compounds with promising magnetic properties.

### Acknowledgements

The work was supported by Russian Science Foundation (project N 14-13-00028) and Grant-in-Aid Scientific Research from JSPS, Japan (23225005 and 26288035).

### Notes and references

- <sup>a</sup>Institute of Problems of Chemical Physics RAS, Chernogolovka, 142432 Russia, FAX: +007-496-522-18-52; E-mail: konarev@icp.ac.ru;  
<sup>b</sup>Institute of Solid State Physics RAS, Chernogolovka, 142432, Russia;  
<sup>c</sup>Research Center for Low Temperature and Materials Sciences, Kyoto University, Kyoto 606-8501, Japan;  
<sup>d</sup>Faculty of Agriculture, Meijo University, 1-501 Shiogamaguchi, Tempaku-ku, Nagoya 468-8502, Japan.
- Electronic Supplementary Information (ESI) available: IR-spectra of **1**, **2** and starting compounds, temperature dependence of g-factor, linewidth and integral intensity of the EPR signal of **2**, CCDC reference numbers are 996945 and 996934 for **1** at 100 and 250 K, respectively and 996969 for **2** at 90 K. For ESI and crystallographic data in CIF or other electronic format see DOI: 10.1039/b000000x/

- 1** F. Bommeli, L. Degiorgi, D. Wachter, Ö. Legeza, A. Jánossy, G. Oszlanyi, O. Chauvet and L. Forró, *Phys. Rev. B*, 1995, **51**, 14794.

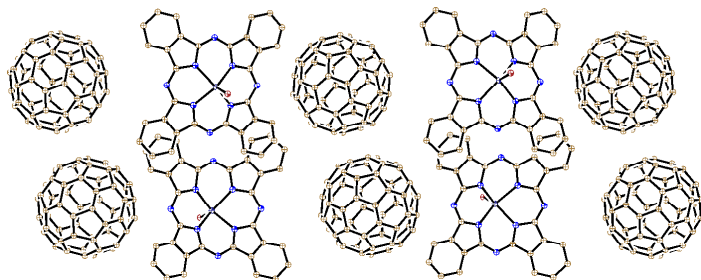
- 2 D. V. Konarev, S. S. Khasanov, A. Otsuka, M. Maesato, G. Saito and R. N. Lyubovskaya, *Angew. Chem. Int. Ed.*, 2010, **49**, 4829.
- 3 A. F. Hebard, M. J. Rosseinsky, R. C. Haddon, D. W. Murphy, S. H. Glarum, T. T. M. Palstra, A. P. Ramirez and A. R. Kortan, *Nature*, 1991, **350**, 600.
- 4 K. Tanigaki, K. Prassides, *J. Mater. Chem.*, 1995, **5**, 1515.
- 5 P. -M. Allemand, K. C. Khemani, A. Koch, F. Wudl, K. Holczer, S. Donovan, G. Grüner and J. D. Thompson, *Science*, 1991, **253**, 301.
- 6 H. Hasegawa, T. Naito, T. Inabe, T. Akutagawa and T. Nakamura, *J. Mater. Chem.* 1998, **8**, 1567.
- 7 T. Inabe and H. Tajima, *Chem. Rev.* 2004, **104**, 5503.
- 8 J. S. Miller, C. Vazquez, J. C. Calabrese, M. L. McLean and A. J. Epstein, *Adv. Mater.*, 1994, **6**, 217.
- 9 E. Tosatti, M. Fabrizio, J. Töbik and G. E. Santoro, *Phys. Rev. Lett.*, 2004, **93**, 117002.
- 10 M. Tahiri, P. Doppelt, J. Fischer and R. Weiss, *Inorg. Chim. Acta*, 1987, **127**, L1.
- 11 H. Huckstadt and H. Homborg, *Z. Anorg. Allg. Chem.*, 1998, **624**, 715.
- 12 D. V. Konarev, S. S. Khasanov, M. Ishikawa, A. Otsuka, H. Yamochi, G. Saito and R. N. Lyubovskaya, *Inorg. Chem.*, 2013, **52**, 3851.
- 13 D. V. Konarev, A. V. Kuzmin, S. S. Khasanov and R. N. Lyubovskaya, *Dalton Trans.*, 2013, **42**, 9870.
- 14 D. V. Konarev, L. V. Zorina, S. S. Khasanov, A. L. Litvinov, A. Otsuka, H. Yamochi, G. Saito and R. N. Lyubovskaya, *Dalton Trans.*, 2013, **42**, 6810.
- 15 E. W. Y. Wong and D. B. Leznoff, *J. Porph. Phth.* 2012, **16**, 154.
- 16 D. V. Konarev, L. V. Zorina, M. Ishikawa, S.S. Khasanov, A. Otsuka, H. Yamochi, G. Saito and R. N. Lyubovskaya, *Cryst. Growth Des.*, 2013, **13**, 4930.
- 17 S. Margadonna, K. Prassides, Y. Iwasa, Y. Taguchi, M. F. Craciun, S. Rogge and A. F. Morpurgo, *Inorg. Chem.*, 2006, **45**, 10472.
- 18 Y. Taguchi, T. Miyake, S. Margadonna, K. Kato, K. Prassides and Y. Iwasa, *J. Am. Chem. Soc.*, 2006, **128**, 3313.
- 19 P. Gargiani, A. Calabrese, C. Mariani and M. G. Betti, *J. Phys. Chem. C*, 2010, **114**, 12258.
- 20 D. V. Konarev, A. V. Kuzmin, S. V. Simonov, S. S. Khasanov and R. N. Lyubovskaya, *J. Porph. Phth.*, 2014, **18**, 87.
- 21 D. V. Konarev, L. V. Zorina, S. S. Khasanov, E. U. Khakimova and R. N. Lyubovskaya, *Russ. Chem. Bull.* 2011, **60**, 1063.
- 22 D. V. Konarev, L. V. Zorina, S. S. Khasanov and R. N. Lyubovskaya, *Dalton Trans.*, 2012, **41**, 9170.
- 23 D. V. Konarev, A. V. Kuzmin, S. V. Simonov, S. S. Khasanov, A. Otsuka, H. Yamochi, G. Saito and R. N. Lyubovskaya, *Dalton Trans.*, 2012, **41**, 13841.
- 24 D. V. Konarev, S. S. Khasanov and R. N. Lyubovskaya, *Coord. Chem. Rev.* 2014, **262**, 16.
- 25 D. V. Konarev, A. V. Kuzmin, S. V. Simonov, S. S. Khasanov, E. I. Yudanov, G. Saito and R. N. Lyubovskaya, *Phys. Chem. Chem. Phys.*, 2013, **15**, 9136.
- 26 T. Picher, R. Winkler and H. Kuzmany, *Phys. Rev. B*, 1994, **49**, 15879.
- 27 V. N. Semkin, N. G. Spitsina, S. Krol and A. Graja, *Chem. Phys. Lett.*, 1996, **256**, 616.
- 28 D. V. Konarev and R. N. Lyubovskaya, *Uspekhi Khimii*, 1999, **68**, 19.
- 29 C. A. Reed and R. D. Bolskar, *Chem. Rev.*, 2000, **100**, 1075.
- 30 D. V. Konarev and R. N. Lyubovskaya, *Russ. Chem. Rev.*, 2012, **81**, 336.
- 31 A. B. P. Lever and P. C. Minor, *Inorg. Chem.*, 1981, **20**, 4015.
- 32 D. V. Konarev, S. S. Khasanov, G. Saito, A. Otsuka, Y. Yoshida and R. N. Lyubovskaya, *J. Am. Chem. Soc.*, 2003, **125**, 10074.
- 33 G. A. Domrachev, Yu. A. Shevelev, V. K. Cherkasov, G. V. Markin, G. K. Fukin, S. Ya. Khorshev, B. S. Kaverin and V. L. Karnatchevich, *Russ. Chem. Bull.*, 2004, **53**, 2056.
- 34 D. V. Konarev, S. S. Khasanov, G. Saito, A. Otsuka and R. N. Lyubovskaya, *J. Mater. Chem.*, 2007, **17**, 4171.
- 35 D. V. Konarev, S. S. Khasanov, G. R. Mukhamadiev, L. V. Zorina, A. Otsuka, H. Yamochi and R. N. Lyubovskaya, *Inorg. Chem.*, 2010, **49**, 3881.
- 36 E. A. Schupak, D. M. Lyubov, E. V. Baranov, G. K. Fukin, O. N. Suvorova and A. A. Trifonov, *Organomet.*, 2010, **29**, 6141.
- 37 N. V. Kozhemyakina, K. Yu. Amsharov, J. Nuss and M. Jansen, *Chem. Eur. J.*, 2011, **17**, 1798.
- 38 D. V. Konarev, S. S. Khasanov, A. Otsuka, H. Yamochi, G. Saito and R. N. Lyubovskaya, *Inorg. Chem.*, 2012, **51**, 3420.
- 39 D. V. Konarev, S. S. Khasanov and R. N. Lyubovskaya, *Russ. Chem. Bull.*, 2007, **56**, 371.
- 40 J. Janczak and R. Kubiak, *Inorg. Chim. Acta*, 1999, **288**, 174.
- 41 D. V. Konarev, A. V. Kuzmin, S. S. Khasanov, A. Otsuka, H. Yamochi, G. Saito and R. N. Lyubovskaya, *New J. Chem.*, 2013, **37**, 2521.
- 42 D. V. Konarev, S. S. Khasanov, A. Otsuka, M. Maesato, M. Uruichi, K. Yakushi, A. Shevchun, H. Yamochi, G. Saito and R. N. Lyubovskaya, *Chem. Eur. J.*, 2014, **20**, 7268.
- 43 D. V.; Konarev, S. S. Khasanov, A. Otsuka, G. Saito, R. N. Lyubovskaya, *Inorg. Chem.* 2007, **46**, 2261.
- 44 D. V. Konarev, A. V. Kuzmin, M. Ishikawa, M. A. Faraonov, S.S. Khasanov, A. Otsuka, H. Yamochi, G. Saito and R. N. Lyubovskaya, *Eur. J. Inorg. Chem.*, 2014, in press. DOI: 10.1002/ejic.201400126.
- 45 D. V. Konarev, S. S. Khasanov, E. I. Yudanov and R. N. Lyubovskaya, *Eur. J. Inorg. Chem.*, 2011, 816.
- 46 R. S. Ruoff, D. Beach, J. Cuomo, T. McGuire, R. L. Whetten and F. Diederich, *J. Phys. Chem.* 1991, **95**, 3457.
- 47 Bruker AXS Inc., Madison, Wisconsin, USA.
- 48 L. J. Farrugia, *J. Appl. Cryst.* 2012, **45**, 849.
- 49 G. M. Sheldrick, *Acta Cryst. A* 2008, **64**, 112.

For Table of Content use only.

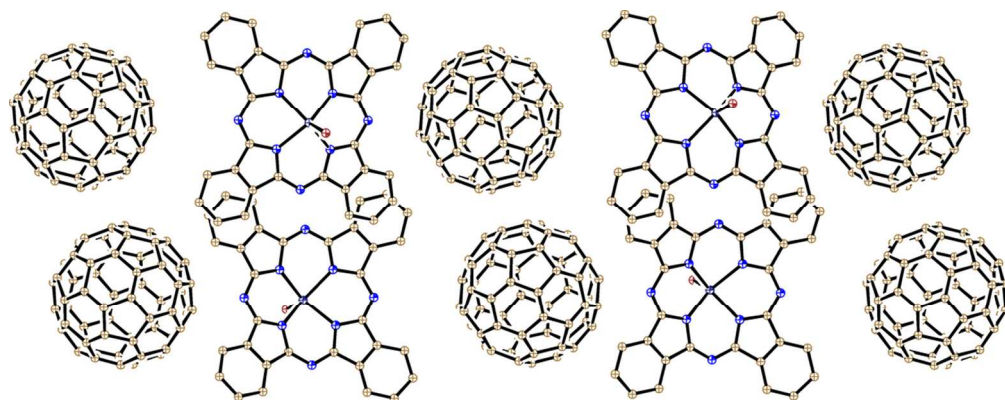
## SYNOPSIS

Salts containing fullerene  $C_{60}$  and indium(III) bromide phthalocyanine (Pc) radical anions,  $(TBA^+)_3(C_{60}^{\bullet-})\{In^{III}(Br)(Pc)^{\bullet-}\}(Br^-) \cdot C_6H_4Cl_2$  (**1**) and  $(TEA^+)_2(C_{60}^{\bullet-})\{In^{III}(Br)(Pc)^{\bullet-}\} \cdot C_6H_4Cl_2 \cdot C_6H_{14}$  (**2**) have been obtained. Effective packing of planar  $In^{III}(Br)(Pc)^{\bullet-}$  and spherical  $C_{60}^{\bullet-}$  is attained by the penetration of fullerenes into the concaved periphery of Pc, resulting in the strong antiferromagnetic coupling of spins in **1** and weaker ferromagnetic coupling of spins in **2**. Molecular structure, optical and magnetic properties of  $In(Br)(Pc)^{\bullet-}$  are presented for the first time.

## GRAPHIC



Interplay between fullerene and phthalocyanine species in  $(TBA^+)_3(C_{60}^{\bullet-})\{In^{III}(Br)(Pc)^{\bullet-}\}(Br^-) \cdot C_6H_4Cl_2$ .



104x40mm (300 x 300 DPI)